



CHEMICAL BATH DEPOSITION OF Cd DOPED LEAD SULPHIDE (PbS) THIN FILMS AND ITS PROBABLE APPLICATION.

¹Goutom Bortamuly, ²Pawan Chetri, ³Santanu Bardaloi.

¹Research Scholar, ²Assistant Professor, ³Scientific Officer

¹Department of Instrumentation & USIC,

¹Gauhati University, Guwahati, India

Abstract: Nanocrystalline thin film of Cd doped PbS is prepared at various concentration of Cd. We have investigated structural and optical properties of the prepared samples. Structural properties are characterized by X-Ray Diffraction, Raman Spectroscopy and SEM-EDS studies. The optical property is studied by UV-Visible spectroscopy. Current vs Voltage (I-V) measurement is also done for all the samples and it reveals that all the samples form ohmic contact. The UV-Visible absorption spectra show that one of the samples possesses high absorption in near infra-red region.

Keywords: PbS-Cd thin films, CBD method, nanocrystalline thin film, structural and optical properties.

I. INTRODUCTION

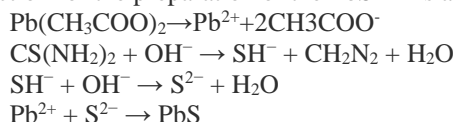
Nanofilms of semiconductors play important roles in advanced scientific technology to improve the overall performance of gadgets made of small chips. It is very important to manage the composition of the films during processing depending upon the different technical requirements. Photovoltaic gadgets often use nanocrystals due to their high performance and low production costs. In recent times polymer compounds in nanoregime [1] are investigated while Lead (Pb) chalcogenide nanocrystals are also actively investigated because they have high Bohr exciton radii (18 nm). CdS and PbS are semiconductors that has sufficient optoelectronic properties, which make it ideal for the manufacture of a wide range of devices such as solar cells, fuel cells, infrared sensors, and so on. Those semiconductors can be obtained using various techniques; one of the most effective methods is chemical bath deposition (CBD) [2-4]. This method requires a very simple and inexpensive tool and deposition can be done on substrates at different temperatures. Lead sulphide (PbS) is black in colour and it is obtained by reaction of Pb^{2+} and S^{2-} ions. The ionic radius of Pb^{2+} and S^{2-} are 1.21 and 1.84 Å respectively [5]. PbS is a semiconductor with a Wurtzite (W) crystal structure of the NaCl type. PbS is important because it has high absorption coefficient which makes it useful in the construction of sensing devices and due to its reflectivity, it is used as a reflective surface in the visible region. An IR detector is a material that changes its properties as it receives radiation. Some physical and chemical techniques have been reported to be almost the method of detecting nanocrystals [6, 7]. PbS is a semiconductor with a bandgap (E_g) = 0.41 eV with continuous absorption in a short wavelength range. However, the increase in E_g is quantified within the range of 0.41- 4.0 eV for 2–20 nm size of nanocrystals [8]. The effect of quantum confinement due to existence of nanocrystals has been investigated in CdS and CdSe semiconductors [9-11]. There is a review of PbS with Cd^{2+} growth through CBD, where there are studies of optical structures and structures [12, 13]. The aim of this work is to find the optimum conditions for the synthesis of PbS with different levels of doping Cd^{2+} ($Cd^{2+} = 0.95$ Å) using CBD and to investigate its optical and structural properties. We will be using the terminology as 0 ml, 2 ml, 4 ml and 6 ml for undoped (0 ml) and Cd doped PbS films respectively. Morphological images using Scanning Electron Microscopy (SEM) were obtained with Voyager II X-ray JEOL JSM-840. The crystalline structure is analyzed using the Nokia D500 diffractometer of the Cu $k\alpha$ line. Optical absorption spectra, measured using the Unicam 8700 Spectrometer.

2. Experiment

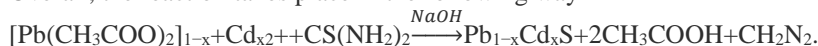
Preparation of polycrystalline PbS thin films on glass substrates at 80°C doped with Cd^{2+} grown by the chemical bath method (CBD) with a pH = 10.5. The parts under the glass were previously soaked in $K_2Cr_2O_7$ / HCl for 24 hours, after which they were rinsed with distilled water. We grew PbS films with four different levels of doping concentration of Cd^{2+} : at 2, 4, 6, and 8 ml respectively. The precursor used to deposit PbS are: 0.01 M of $Pb(CH_3COO)_2$, 0.5 M of NaOH, 1.5 M of NH_4NO_3 and 0.2 M of $SC(NH_2)_2$. The doping solution of $CdCl_2$ used at 0.02, 0.04, 0.06 and 0.08 M respectively is slowly incorporated into the reaction component

while growing PbS film. All solutions used were water-repellent. The films were silver-gray, cohesive, polycrystalline and adhering well to the substrate.

The reaction for the preparation of the PbS films are as given below:



Overall, the reaction takes place in the following way-

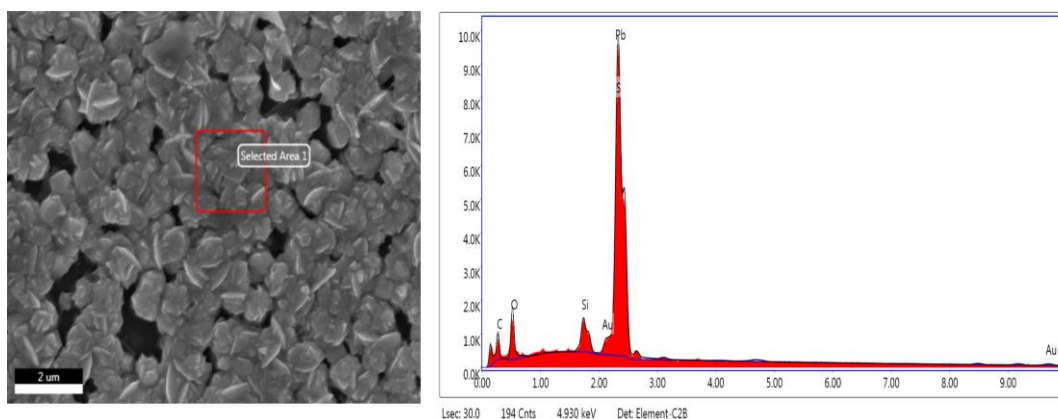


3. Results and discussion

3.1 Scanning Electron Microscopy (SEM)

Morphologies of nanocrystalline PbS and Cd-doped PbS small films are investigated using SEM as shown in Fig. 1. PbS nanocrystalline films are undetectable and doped, prepared using chemical classification of their size and morphology. The small prepared films had the same surface morphology over the entire lower glass and were of good quality. Cd doping has caused significant changes in surface morphology and size. The surface of the pure PbS film was similar and filled with nanocrystallite, which looked randomly directed and showed an unusual shape. When a Cd is inserted into the PbS lattice, grain size and film thickness decrease. This variation is due to nucleation and coalescence. In general, nucleation and coalescence alter grain growth by moving the grain boundaries. This process depends very much on many other factors, such as precursors, type of solvent, solution supply rate, installation temperature etc. The current case may be due to the effects of the Cd solution. The doped film shows small particles that play a role in crystal concentrations, thus showing the nanocrystalline nature of Cd-doped PbS small films.

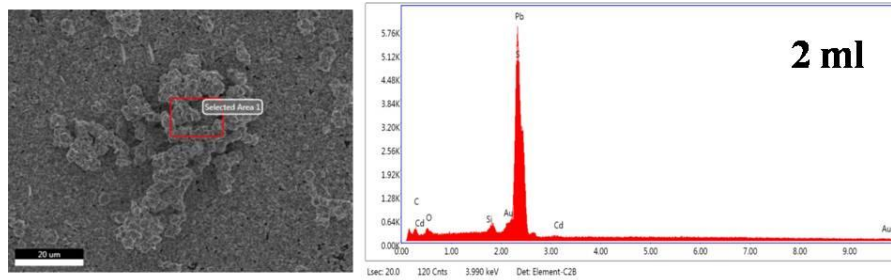
EDX exhibition of PbS / Undoped films and PbS / Cd shown in fig1 (a) - (d). It is evident from Fig. 1 (a) that the PbS / Undoped film is not stoichiometric with Pb spaces. Each Pb space forms two holes in the valence band making it a p-type semiconductor. [14] Provides electronic standards that remain above the valence band. Figure 1 (b) - (d) shows an increase in Cd content. It ensures the installation of the Cd in the PbS tank. A certain amount of Oxygen was found in the films. This is due to the absorption of O²⁻ and OH⁻ ions. Another pollution found in films is carbon. The source of this substance may have been caused by CH₂N₂ which is a decaying form of thiourea.



Element	Weight %	Atomic %
C K	5.51	25.77
O K	8.52	29.90
Si K	2.60	5.19
Au M	3.21	0.92
S K	11.15	19.53
Pb M	69.00	18.70

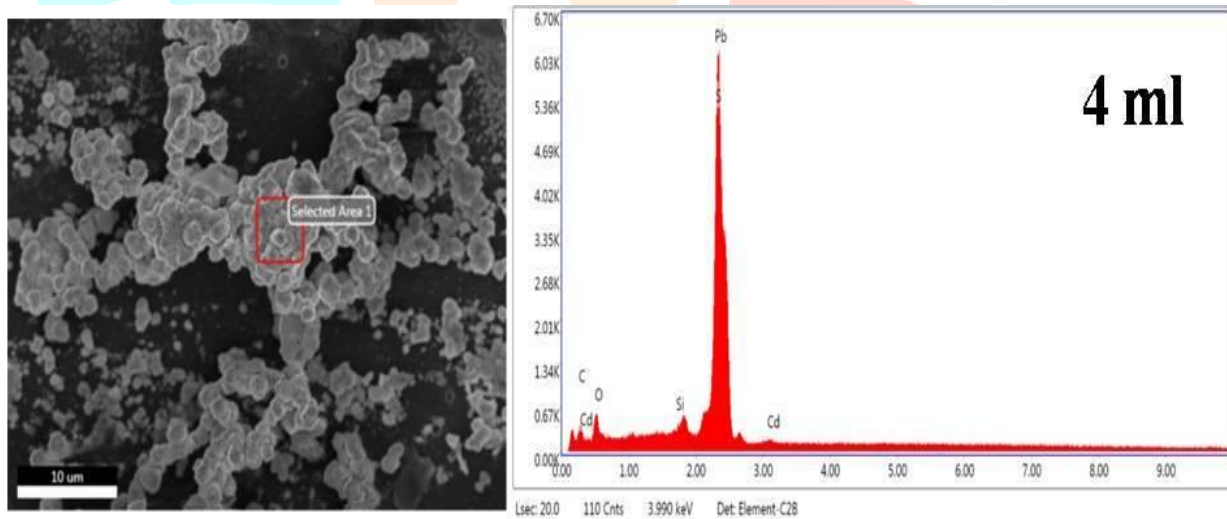
(a)

Fig. 1(a): SEM micrograph of Undoped PbS Thin Film.



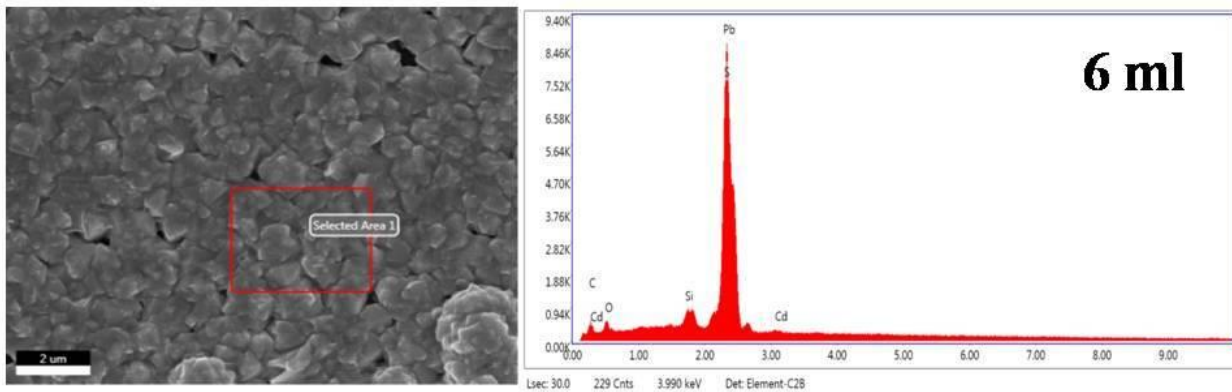
Element	Weight %	Atomic %
CK	4.47	26.75
OK	3.46	15.55
SiK	0.16	0.40
AuM	3.77	1.37
SK	13.39	29.99
PbM	74.68	25.89
CdL	0.07	0.05

Fig. 1(b): SEM micrograph of 2 ml Cd doped PbS Thin Film.



Element	Weight %	Atomic %
CK	4.24	23.51
OK	5.57	23.19
SiK	0.63	1.49
SK	13.07	27.16
PbM	76.28	24.52
CdL	0.21	0.12

Fig. 1(c): SEM micrograph of 4 ml Cd doped PbS Thin Film.



Element	Weight %	Atomic %
SK	13.94	51.09
PbM	85.83	48.67
CdL	0.23	0.24

3.2 X-ray diffraction (XRD)

Fig. 2 shows XRD patterns of undoped and doped thin films of different concentrations of Cd. It shows two angular peaks at $2\theta = [27.25, 28.49]$, which may be due to monoclinic phase of PbO (JCPDS 019-0697), and the other peak at $2\theta = [34.04]$ can be due to orthorhombic phase of PbO (JCPDS levels 052-0772).

In order to explain the degree of the undoped and doped PbS films preferred orientation, the texture coefficients (TC) of (111) and (200) planes were represented by the Harris method in the following formula

$$TC = \frac{I_m}{I_s} \left[\frac{1}{n} \sum \frac{I_m}{I_s} \right]^{-1}$$

Where I_m is the measured intensity and I_s , the standard intensity of the peak corresponding to the (hkl) plane and n is the number of diffraction peaks. We have considered (111) and (200) peaks as the reference in this calculation. The values of TC for (111) and (200) of undoped and doped films were found to be 25.99% and 30.13% respectively. Hence it is observed that the plane (200) has a high texture coefficient, indicating that the prepared films have preferential orientation towards the (200).

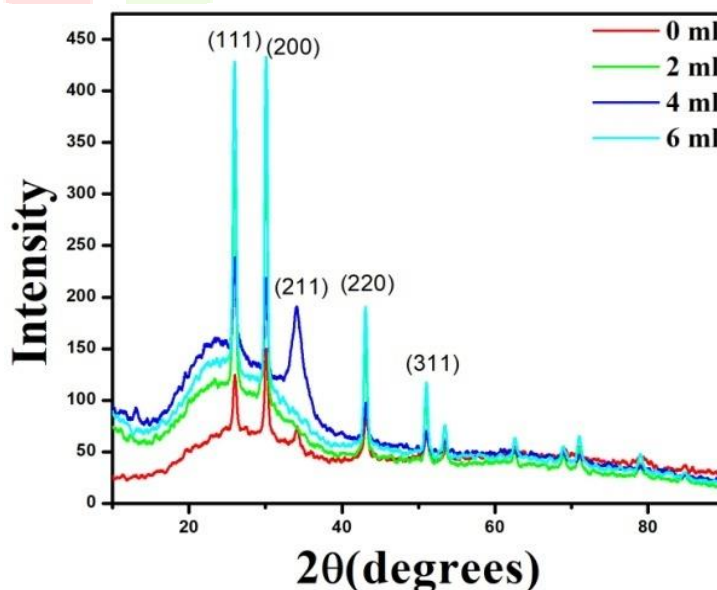


Fig. 2: XRD pattern of undoped and doped Thin Films.

3.3 Scherrer's Formula

The average crystallite size (D) of the nanocrystalline PbS thin films are obtained by using Scherrer's equation [15]:

$$D = \frac{0.94 \lambda}{\beta \cos \theta}$$

Where λ is the wavelength of x-ray used, β is the FWHM of the peak corresponding to a particular set of crystal plane and θ is Bragg angle. The above formula gives the average crystallite size in a direction perpendicular to a respective plane. In Table 1; we have observed that the crystallite size decreases as the doping concentration increases. This can be attributed to the defects increased in the system due to doping such as point defects or lattice defects. The size of Cd^{2+} is lesser than the host Pb^{2+} which increases the chances of perfect substitution. This reduces the probability of forming Cd cluster on the surface.

Table 1: Crystallite Size, Band gap and Strain

Concentration(ml)	Crystallite Size(D) nm	Band gap(eV)	Strain, $\epsilon \times 10^{-3}$
0	34.76	3.16	0.997
2	30.96	3.34	1.119
4	27.62	3.66	1.254
6	23.68	3.35	1.463

3.4 Optical properties of the Films by UV-Visible Spectrophotometer

The optical absorbance (A) variation of the films against the wavelength is shown in Fig.3. It is evident that films prepared with Cd concentration of 6ml show high absorption in the IR region. It may be due to the large number of impurity states formed within the band gap of 6 ml sample. These impurity states lead to increase in absorption tail which extends upto IR range and hence absorbance increases from 700 nm to 900 nm. The sharp rise in the absorbance of all the samples in the UV region indicates the distribution of a small size of nanoparticles. As shown in Fig. 3; absorbance is reduced as the volume of Cadmium dopant increases. A. M. Ahmed et. al. note the similar behavior in Cr-doped PbS nanofilms [16]. The absorption edge is gradually changed from the longest length (near the IR region) to the shorter length (visible region) in doped films, showing an increase in their bandgap value. This change is due to a decrease in the crystallite size as a result of defects introduced by doping.

The film clarity of pure PbS less than 700 nm is increased by the Cd doping ratio as shown in Fig. 4. The reason for the transmission is what is seen in the doped films in the UV / Visible light region may be due to the evolution of the free carrier concentrations.

Depending on the recorded absorbance (A) and film size (t), the absorption coefficient (α) is calculated using the relationship:

$$\alpha = 2.303 A / t$$

The type of change associated with the PbS band structure can be identified using the following relationship:

$$(\alpha h\nu)^2 = K (h\nu - E_g)$$

There, K is energy independent constant, h is Planck constant, ν photon frequency, E_g the optical band gap between the bottom of the conduction band and above the valence band and α is the absorption coefficient.

The value of the bandgap can be calculated from the vertical line of $(\alpha h\nu)^2$ compared to the curve crossing the $h\nu$ axis as shown in Fig. 5. Depending on the effect of quantum confinement, the expansion of the band gap occurs due to a decrease in the crystallite size calculated from XRD data as shown in Table 1.6 ml sample shows a sudden decrease in band gap against the traditional quantum confinement effect. The decrease in E_g value of 6 ml sample may be due to the Moss-Burstein effect, where the dopant element increases the electron density of the conduction band thus raising the Fermi level [17].

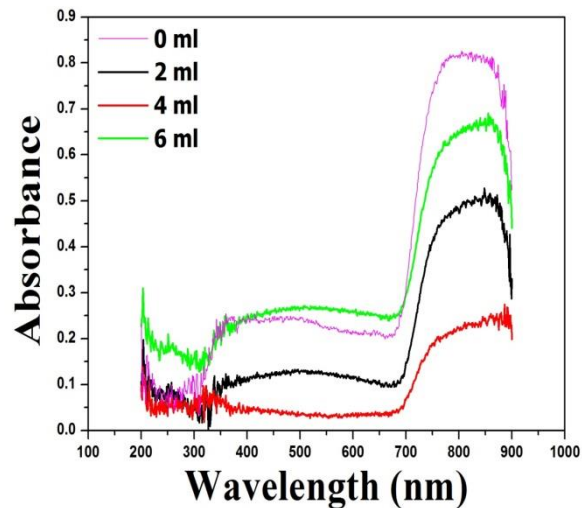


Fig 3: Absorption Spectra of undoped and doped thin films.

The Gaussian plot of Fig. 3 shows the presence of two peaks in each of the sample. The wavelength, absorbance and percentage of fitting are given in Table 2. The absorbance is measured after making a baseline correction for Fig.3. We have seen that 0 ml sample shows the maximum absorbance in the visible region while 6 ml sample have the maximum absorbance in the IR region.

Table 2: Wavelength, Absorbance and Fitted Parameter (R^2)

Concentration	Wavelength(nm)	Absorbance	Fitted Parameter
0 ml	464	0.2007	0.97
	818	0.6709	
2 ml	518	0.1524	0.98
	832	0.6508	
4 ml	156	0.1652	0.94
	843	0.2522	
6 ml	516	0.1730	0.98
	831	0.8115	

3.5 Raman Spectroscopy

Raman Spectroscopy is a non-invasive procedure used to easily provide information about crystal formation of films. In general, the crystal shows the sharp and strong peaks of the Raman while the amorphous sample exhibits broad and fragile Raman peaks. [18]. The Raman Spectra of all the prepared samples is displayed in Fig. 4. In 0 ml sample, the peaks were seen at 92,138,438 and 973 cm^{-1} . Raman height at 92 cm^{-1} may be due to the combination of longitudinal and transverse acoustic phonon mode (LA + TA) in a small PbS film. This mode is also reported by Ovsyannikov et al. [19,20]. The band located at 138 cm^{-1} may come from a combination of transverse acoustic and optical (TA + TO) phonon mode which can be compared with the effect of Ovsyannikov et al. The maximum value of 438 cm^{-1} can be calculated in the longitudinal optical phonon mode [21]. A slightly higher height of 973 cm^{-1} may be related to the PbSO_4 phase [22]. In 2ml sample, peaks were found at 99 and 1047 cm^{-1} . The maximum value of 99 cm^{-1} represents the LA + TA mode. A maximum value of 1047 cm^{-1} can be assigned to $3\text{PbO} \cdot \text{PbSO}_4 \cdot \text{H}_2\text{O}$ according to Lara et al. [23]. At 4ml sample, the peaks focus on 88,159,197 and 472 cm^{-1} respectively. The first two peaks are due to LA + TA and TA + TO phonon mode respectively. The third highest value can be based on LO + TO mode and 472 cm^{-1} can appear on the first phonon mode. At 6ml sample, the peaks are found on 99 and 162 cm^{-1} . The initial height can be caused by the LA + TA mode while the other is due to the TA + TO phonon mode.

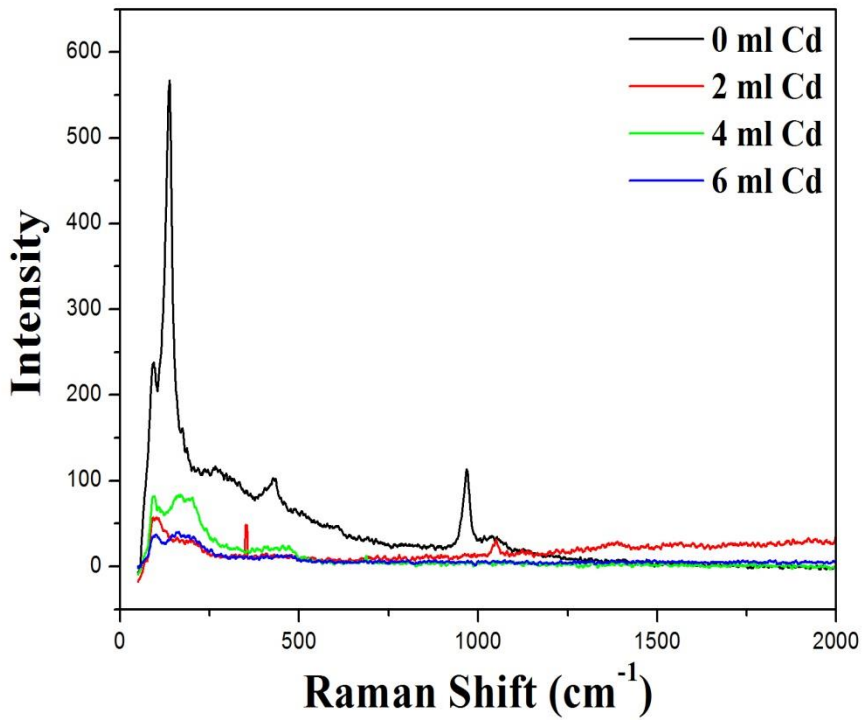


Fig 4: Raman Spectra of un-doped and doped thin films.

3.6 Current-Voltage Characteristics of the Films

Fig. 5 shows the voltage-current characteristics of all the prepared samples. It is evident that the variation in current with voltage indicates ohmic contact. The highest conductivity is found in 2 ml sample while the minimum conductivity is achieved in 6 ml sample. Decreased electrical conductivity in high Cd concentrations may be related to increased film mass [24,25]. The reason for this behaviour is a crystalline degradation that leads to a decrease in the size of the crystallite with increasing defects. It is well known that although with a 6ml sample, Pb is rich; it shows a small density that may be due to the omission of the existing Pb atoms as PbO in the film but not as a Pb element. Table 3 shows the conductivity calculated for each prepared sample.

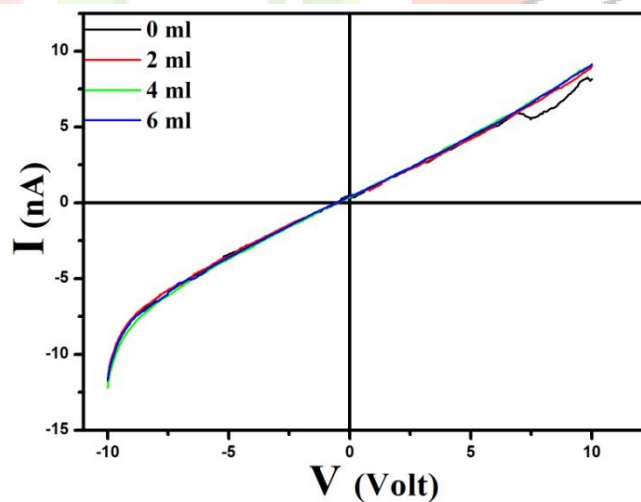


Fig 5: Current-Voltage Characteristics of all the samples

Table 3: Sample and Conductivity

Concentration(ml)	Conductivity(Ωcm^{-1})
0 ml	9.85×10^{-10}
2 ml	10.4×10^{-10}
4 ml	8.48×10^{-10}
6 ml	7.78×10^{-10}

4. Conclusion

In this study, PbS and Cd-doped PbS nanocrystalline films were successfully prepared using a chemical deposition method. Films raised under these conditions are well documented. From optical absorption, high absorption in the IR region by 6 ml of Cd-doped suggests that it may be useful for IR detector. We have successfully tuned the optical band gap for PbS films prepared for a wide range and thus made it a probable high-performance photovoltaic applications. XRD and EDX analysis confirms the formation of nanocrystalline Cd doped PbS films.

5. References

- [1] W.U. Huynh, J.J. Dittmer and A.P. Alivisatos. 2002. Hybrid Nanorod-Polymer Solar Cells, 295(5564): 2425-2427
- [2] D.K.Kaur, K.L.Pandya and J. Chopra. 1980. Photovoltaic effect of Chemically deposited $\text{Cu}_2\text{S}/\text{CdSi}$ heterojunctions. *Electrochemical Soc.*, 127: 943-946
- [3] P.K.Nair and M.T.S.Nair. 1990. The deposition of highly uniform and adhesive nanocrystalline PbS film from solution. *Phys. D: Appl. Phys.*, 23: 150-154
- [4] R.K.Joshi, A.Kanjilal and H.K.Sehgal. 2004. Solution Grown PbS Nanoparticle Films. *Applied Surface Science*, 221: 43-47
- [5] G.A.Kitaev, A.A.Uritskaya and S.G.Mokrushin. 1965. $\text{ZnO}/\text{CdS}/\text{CuInSe}_2$ Photovoltaic Cell fabricated using Chemical Bath Deposited CdS buffer layer. *Russ. J. Phys. Chem.* 39: 1101
- [6] J. Xu, D.H.Cui, T. Zhu, G.Paradee, Z.Q.Liang and Q.Wang. 2006. Synthesis and Surface modification of PbSe/PbS Core shells Nanocrystals for potential device applications. *Nanotechnology*. 17: 5428-5434
- [7] H.Q.Cao, G.Z.Wang, S.H.Zhang and X.R.Zhang. 2006. Growth and Photoluminescence properties of PbS Nanocubes. *Nanotechnology*. 17: 3280-3287
- [8] R.K.Joshi, A.Kanjilal and H.K.Sehgal. 2003. Size dependence of optical properties in solution grown $\text{Pb}_{1-x}\text{FexS}$ Nanoparticle Films. *Nanotechnology*. 14: 809-812
- [9] N.S.Kozhevnikova, A.A.Rempel, F.Hergert and A.Mageruli. 2009. Structural Study of the initial grow of Nanocrystalline CdS Thin Films in a chemical bath. *Thin Solid Films*. 517: 2586-2589
- [10] A.R.Marquez, M.R.Falfan, R.L.Morales, O.P.Moreno and O.Z.Angel. 2001. Quantum Confinement and Crystalline structure of CdSe Nanocrystalline Films. *Phys. Stat. Sol.* 188: 1059-1063
- [11] S.Bhushan, M.Mukherjee and P.Bose. 2002. Electro-Optical Studies in Chemically Deposited La/Nd doped (Cd-Pb)S Films. *J. Mat. Sci. Electro.* 13: 581-584
- [12] H.M.Upadhyaya and S.Chandra. 1994. Chemical bath deposition of band gap tailored $\text{Cd}_x\text{Pb}_{1-x}\text{S}$ Films. *J. Mat. Sci.* 29: 2374-2380
- [13] M.A.Mohammed, A.M.Mousa and J.Ponpon. 2009. Optical and Optoelectric Properties of PbCdS ternary thin films deposited by CBD. *J. Semicon. Tech. Sci.* 9: 117-122
- [14] J.I.Pankove. 1975. *Optical Processes in Semiconductor*. Dover Publications Inc.
- [15] Yu Jun Yang and Hu Shengshui. 2008. The deposition of highly uniform and adhesive nanocrystalline PbS film from solution. *Thin Solid Films*. 516(18): 6048-6051
- [16] H.Jiabin, L.Weil and W.Teng. 2019. Effect of Cr doping Concentration on the Structural, Optical and Electrical Properties of Lead Sulphide (PbS) Nanofilms. *Coating*. 9: 376
- [17] K.Usharani, A.R.Balun, V.S.Nagarethinam and M.Suganya. 2015. Characteristics analysis on the physical properties of Nanostructured Mg-doped CdO Thin Films-doping concentration effect. *Prog. Nat. Sci: Mater. Int.* 25: 251
- [18] H.Sarma, D. Chakraborty and K.C.Sarma. 2017. X-ray analysis of Cadmium Oxide Nanostructured Films Synthesized with different precursor molarities by Silar method. *Asian Journal of Chemistry*. 29: 2005-2010
- [19] E. Sarica and V.Bilgin. 2019. The Effect of substrate temperature on the structure and morphologies of PbS Thin Films deposited by Ultrasonic Spray analysis. *Journal of Innovative Science and Engineering*. 3(2): 66
- [20] Chernyshova IV. 2001. Anodic Processes on a galena (PbS) electrode in the presence of n-butyl Xanthate studied FTIR Spectroelectrochemically. *JPC B*. 105: 8185-8191
- [21] S.V.Ovsyannikov, V.V.Shchennikov, A.Cantarero, A.Cros and A.N.Titov. 2007. *Mater. Sci. Eng. A*. 462: 422
- [22] R.Sherwin, R.J.H.Clark, R.Lauck and M.Cardona. 2005. *Solid State Commun.* 134: 565
- [23] E.Schreck, V.Dappe, G.Sarret, S.Sobanska, D.Nowak et. al. 2014. *Sci. Total Environ.* 667: 476-477
- [24] R.H.Lara, R. Briones, M.G.Monroy et. al. 2011. *Sci. Total Environ.* 409: 3971
- [25] T.L.Remadevi and K.C.Preetha. 2012. *J. Mater. Sci: Mater Electron.* 12: 53